HHS Public Access

Author manuscript

Adv Mater. Author manuscript; available in PMC 2017 October 01.

Published in final edited form as:

Adv Mater. 2016 October ; 28(39): 8675–8680. doi:10.1002/adma.201602606.

Supramolecular metallo-bioadhesive for minimally invasive use

Dr. Seonki Hong,
Center for Systems Biology, Massachusetts General Hospital 185 Cambridge St., CPZN 5206, Boston, MA 02114

David Pirovich,
Center for Systems Biology, Massachusetts General Hospital 185 Cambridge St., CPZN 5206, Boston, MA 02114

Dr. Aoife Kilcoyne,
Center for Systems Biology, Massachusetts General Hospital 185 Cambridge St., CPZN 5206, Boston, MA 02114; Division of Interventional Radiology, Massachusetts General Hospital 55 Fruit St., Boston, MA 02114

Dr. Chen-Han Huang,
Center for Systems Biology, Massachusetts General Hospital 185 Cambridge St., CPZN 5206, Boston, MA 02114

Prof. Dr. Hakho Lee, and
Center for Systems Biology, Massachusetts General Hospital 185 Cambridge St., CPZN 5206, Boston, MA 02114

Prof. Dr. Ralph Weissleder*
Center for Systems Biology, Massachusetts General Hospital 185 Cambridge St., CPZN 5206, Boston, MA 02114; Division of Interventional Radiology, Massachusetts General Hospital 55 Fruit St., Boston, MA 02114; Department of Systems Biology, Harvard Medical School 200 Longwood Ave., Boston, MA 02115

Graphical abstract

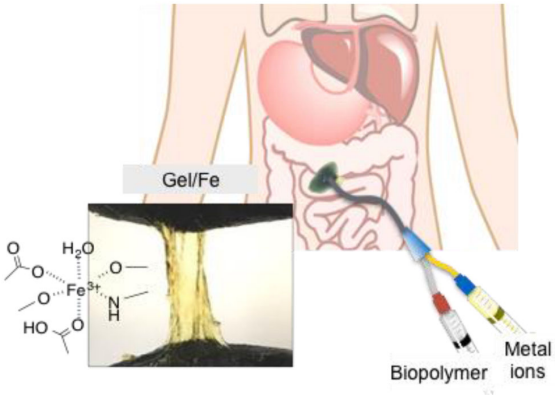

*Prof. Dr. R. Weissleder, rweissleder@mgh.harvard.edu.

Keywords

tissue adhesive; sealant; metal-ligand complexation; catechol-conjugated polymers; surgery; image-guided intervention

Despite remarkable advances in image-guided intervention, endoscopic approaches and robotic surgical techniques, chronic organ leaks and fistulas secondary to inflammatory disease, trauma or prior surgery remain difficult to treat. Examples include pancreatic,[1] biliary,[2] colorectal,[3] bronchopleural[4] and genitourinary fistulas[5] among many others. While a major focus has been on preventing such fistulas, once established, their treatment can be lengthy and complex, thereby adding to the financial healthcare burden. Since repeat surgery is frequently too invasive and not definitive, alternatives are required. Tissue sealants with adhesive properties delivered by image-guided intervention have the potential to play an important therapeutic role, but existing materials are suboptimal. For example, available adhesives have a success rate of only 60-75% in treating fistulas.[6,7]

A limited number of sealants are in clinical use, often for hemostasis or vascular repair. For example, fibrin glue sealants are tissue adhesives composed of human fibrinogen and thrombin that were originally developed for tissue sealing, wound closure and hemostasis. In prospective trials, however, fibrin-based glues did not show a benefit in sealing high-output fistulas, mainly due to the glues' weak adhesive strength.[8,9] Methacrylate adhesives ("superglue") are strong adhesives commonly used as Dermabond for wound closure,[10] polymethyl methacryclate in kyphoplasty[11] or histo-acryl glue in cardiac surgery.[12] Methacrylates have also been used experimentally in some fistulas,[13] but their application can be technically challenging, especially with catheters, as glues polymerize during delivery. Finally, Onyx is a liquid embolization material, composed of ethylene-vinyl alcohol, dimethylsulfoxide (DMSO) and tantalum powder, that forms a non-adhesive cast upon DMSO diffusion. Onyx is approved for embolization of arteriovenous malformations but has also been used experimentally in fistulas.[14] Most of the materials described above are expensive, particularly when large fistulas or cavities are to be treated. For example, material costs for repairing a biliary leak can easily reach tens of thousands of dollars.

There is thus a clear need for new low-cost sealing materials with improved functional properties and ease of use. In an ideal scenario, these materials should be adhesive, space filling, biocompatible, reversible on demand, slowly biodegradable, nontoxic and inexpensive. With the intention of creating such materials for interventional procedures, we considered basing such materials on Gelfoam, a commonly used surgical product currently without adhesive properties. Gelfoam is a gelatin sponge originally developed for hemostatic applications and is FDA approved. From this starting point, we sought to impart gelatin derivatives with adhesive properties through chemical cross-linking. Unexpectedly, we found that metal complexation can be used to render gelatin derivatives adhesive. Inspired by this observation, we conducted more in-depth experiments on the material's properties. Here we present data on two novel metallo-bioadhesives to be used as tissue sealants in minimally invasive procedures.

Fig. 1a illustrates representative structures of gelatin (Gel) and its dopamine-modified version (GelDA). The GelDA material was developed to increase the water-resistant adhesion by mimicking the adhesive proteins in mussels.[15] GelDA was synthesized via an EDC coupling reaction between the carboxyl groups in Gel and the amine group of dopamine (Fig. 1a). The degree of conjugation of GelDA was approximately 7-8 catechols per each Gel backbone, as confirmed by ultraviolet-visible (UV-vis) spectroscopy and nuclear magnetic resonance (NMR) analysis (Fig. S1). Adding $FeCl_3$ to Gel or GelDA forms hexavalent Fe complexes, effectively cross-linking strands or forming a metallo-bioadhesive with tissue proteins (Fig. 1b). The formation of Fe-O bonds was confirmed by Fourier transform infrared spectroscopy (FT-IR), which showed a strong band at 538 cm^{-1} following metal complexation (Fig. S2). This band is characteristic of metal-oxygen stretching absorbance.[16,17] Cohesion and/or adhesion properties are primarily governed by the stoichiometric ratio between protein functional groups and metal ions. Ideal cohesive conditions are achieved when all Fe^{3+} ions coordinate with the functional groups of the biopolymer (3rd state in Fig. S3a). Through titration experiments of rheological studies, we determined that 100 mM of Fe^{3+} on 15% (w/v) Gel or GelDA achieved this condition (Fig. S3b). At higher Fe^{3+} concentrations, adhesion increases as excess Fe^{3+} forms cross-links between polymer and tissue proteins (Fig. 1c and 4th state in Fig. S3a. Through titration experiments of the lab shear strength shown in Fig. 2a, we determined that 500 mM of Fe^{3+} showed an ideal performance as a tissue sealant (assuming 15% w/v gel). Since both initial solutions are non-viscous, they can easily be delivered via dual lumen microcatheters to form an adhesive upon contact (Fig. 1d).

The adhesive strengths of Gel/Fe and GelDA/Fe were measured by lab shear testing on porcine skin under natural, moist conditions. The lab shear strength of Gel/Fe was greatest at 500 mM of $FeCl_3$ where the maximum values reached 4 N/cm^2 (Fig. 2a**, white bar**). At lower iron concentrations, the lab shear strength was ~1 N/cm^2, similar to fibrin glue.[18] GelDA showed slightly better tissue sealing performance over a wider range of $FeCl_3$ (Fig. 2a**, blue bar**).

We next determined how fast the bioadhesives formed. We spiked Gel and GelDA with florescence dye and measured changes in florescence polarization during gelation. The polarization value increased as the mixture (Gel/Fe or GelDA/Fe) solidified and concomitantly decreased dye mobility. The gelation was fast and concluded within 30 seconds (Fig. 2b). In medical practice, it is advantageous to have reversible adhesive systems to minimize serious complications when adhesives inadvertently enter spaces for which they are not meant. For example, if adhesive plugs were formed in the intravascular space, they could lead to catastrophic embolic events. To investigate the rapid dissolution of adhesives, in case of inappropriate placement, we tested two approaches: the use of enzymes (collagenase, urokinase) for bioadhesive breakdown and the use of iron chelators (deferoxamine, DFO) to disrupt Fe-biopolymer coordination. Collagenase effectively dissolved both Gel/Fe and GelDA/Fe complexes (10 min). Urokinase, on the other hand, was less effective than collagenase, taking more time to dissolve Gel/Fe and having negligible effect on GelDA/Fe (Fig. S4a). In contrast to these enzymes, the Fe-chelating agent DFO was far superior in dissolving adhesives; both Gel/Fe and GelDA/Fe were completely

dissolved within 1 min (Fig. 2c). Such fast kinetics could be attributed to much more favorable binding between DFO and Fe (binding constant, log K_1 = 30.6)[19] that replaces the weaker Fe-biopolymer coordination (log K_1 = 4.3)[20] (Fig. S4b). In an *ex vivo* study of tubulo-vascular injury, we successfully sealed a leak with GelDA/Fe and then dissolved the adhesive by locally administering DFO (Fig. S5).

Next, we monitored bio-degradation of the adhesives in physiological conditions. We implanted pre-formed Gel/Fe and GelDA/Fe complexes in subcutaneous areas on the backs of mice, and the implanted materials were harvested and weighed at 3 and 23 days after implantation. Both materials were completely degraded 23 days after implantation (Fig. 2d). Gel/Fe had a half-life of 2 days, whereas GelDA/Fe showed a longer half-life (7 days), presumably because of the covalent nature of cross-linking induced by Fe^{3+} release.[21] During the degradation, slow release of Fe^{3+} will occur which is bioabsorbed by iron-binding proteins (transferrin, lactoferrin and ferritin) and incorporated into the body's iron pathway.[22] The total amount of Fe^{3+} is less than 68 mg for 1 mL of Gel/Fe complex, which is less than the amounts of iron given for typical iron replacement therapy. Neither Gel nor GelDA elicited acute cytotoxicity up to 7 days (tested in 3T3 fibroblasts; Fig. 2e). Using the PrestoBlue assay, we furthermore confirmed that cells proliferated in the presence of biopolymers (Fig. S6). Furthermore, serial tissue histology showed no untoward effects (e.g., inflammation) from the implanted materials. Residual Gel/Fe and GelDA/Fe depots were detectable by histology given their slightly brown color (Fig. S7 and 2f). One month after implantations no residual materials could be detected, nor was there fibrosis or residual inflammation. Both Gel/Fe and GelDA/Fe gels had characteristics that enabled cells to adhere and grow on the materials (Fig. S8). We observed time depended attachments and cell proliferation and adhesion over the 7 day observation period. To further investigate the structure of the gels we performed scanning electron microscopy (SEM) (Fig. S9). Image analysis showed that the materials had irregular surfaces, large clefts and pore structures. These features would be conducive to cell attachment, as absorbed in similar biogels.[23,24]

We next used the metallo-bioadhesive to treat an iatrogenic injury in a mouse model. Specifically, we created a surgical wound in the mouse uterine horn (Fig. 3a). Trypan blue injected through the uterus leaked, confirming the injury. For the treatment group, we applied GelDA and $FeCl_3$ simultaneously at the incision site. The pre-gel is of low viscosity to permeate through injured tissue before the rapid gelation with in minutes. This spreading allows extremely effective tissue sealing and contributes to the success of procedures. Five minutes after the glue application, we re-injected the test dye again; no leak was observed from the repair site, which demonstrated effective wound sealing (Fig. 3b and Video S1).

As traditional surgical approaches are replaced with less invasive procedures, the demand for new adhesive sealants concomitantly increases. These new materials should bind efficiently to tissue under wet conditions, be biocompatible and work well in conjunction with modern therapeutic interventions. In the search for ideal sealants, particularly those that can be delivered via small-bore catheter systems, we started to experiment with FDA-approved agents that have extensive clinical safety and efficacy data. We hypothesized that certain gelatin derivatives could be ionically cross-linked to yield stable 3-dimensional polymeric networks. In this work, we show the mechanical and adhesive properties of simple metallo-

bioadhesives that are tunable by stoichiometric complexation between Fe^{3+} and multi-ligands in gelatin (amine, hydroxyl and carboxyl groups). Importantly, a 20% Fe^{3+} solution is medically approved as a hemostatic under the name of Monsel's solution, while Gelfoam is in routine clinical use.

Ionic complexation between metal ions and various polymers (and tissue proteins) is well established. For example, a multi-stimuli-responsive supramolecular hydrogel based on the reversible interaction between silver (Ag^+) ions and functional groups of chitosan has been reported.[25] Leibler *et al.* have described aqueous solutions of nanoparticles as adhesives for sealing tissues.[26,27] Furthermore, the complexation of metal ions with catechol-conjugated biopolymers has been used to control the viscoelastic mechanics of soft polymeric materials. Polyethylene glycol (PEG) with different ligands (histidine and catechol) have been complexed with Ni^+.[28] Despite these reports, we were surprised by the paucity of literature on iron complexed protein networks, as this approach appears remarkably simple, biocompatible and natural.

These metallo-bioadhesives have several of advantages. First, the starting materials are not viscous and can be easily delivered through microcatheters and other delivery systems often used in interventional procedures. Second, complexation occurs within minutes *in vivo* and results in a stable bioadhesive with the half-life of days to weeks, depending on volume. Third, Fe^{3+} functions as a hemostatic (i.e. it stops bleeding) in addition to cross-linking the gelatin. Fourth, the materials are safe for implantation with negligible tissue toxicity. This is not entirely surprising given the wide use of gelatins in medicine. Finally, the ingredients are relatively inexpensive, an important consideration when large areas or cavities need to be repaired.

The ability to fabricate robust bioadhesives enables/actuates a number of future directions and applications. For example, the materials seem suited for repairing recalcitrant biliary or urinary leaks, which may lead to a new class of alternative repairs and simpler surgery. Further, the materials could be used during organ biopsies to reduce bleeding complications. Precision medicine often requires repeat biopsies, and new efficient bioadhesives may be able to reduce complication rates and recovery times. Finally, pre-coated materials such as detachable coils, stents and other implantables may be used to hasten incorporation and better match the physiological properties of surrounding tissues.

Experimental

Dopamine-conjugate gelatin (GelDA) synthesis and characterization

800 mg of gelatin (Gel) (275 Bloom, from porcine, kindly donated by GELITA®) was dissolved in 80 mL of 50 mM MES buffer (Sigma Aldrich) at 50 °C for 1 hr with N_2 bubbling. Then, 845 mg of N-(3-Dimethylaminopropyl)-N'-ethylcarbodiimide hydrochloride (EDC, 6 eq to the total amount of carboxyl group in the solution, Sigma Aldrich), 626 mg of N-hydroxysuccinimide (NHS, 6 eq, Sigma Aldrich) and 516 mg of dopamine hydrochloride (3 eq, Sigma Aldrich) were serially added to the solution at 50 °C. The pH of the solution was quickly adjusted to 5 by adding 5 M HCl. The solution was kept at 50 °C for 6 hrs under N_2 stream and dialyzed (Spectra/Por standard RC dialysis tubing, MWCO = 12-14 kDa)

against distilled water containing 20 mM of NaCl and 833 μM of HCl for 2 days at 40 °C followed by pure distilled water for 3 hrs to remove NaCl. The purified GelDA was collected by lyophilization and stored at −20 °C for further use. Dopamine conjugation was confirmed by ^{1}H-NMR (Bruker AscendTM 400), and the degree of conjugation (DOC) of dopamine on Gel backbone was analyzed by UV-vis spectroscopy (Tecan Safire2). The absorbance of GelDA (10 mg/mL in distilled water) at 280 nm of wavelength was measured and compared with the absorbance of dopamine solutions with known concentrations.

Preparation of Gel or GelDA with iron (Fe^{3+}) complex

15% (w/v) Gel or GelDA solution was prepared by dissolving 15 mg of Gel or GelDA in 100 μL of 1XPBS (pH 7.4, Corning®) at 40 °C for 30 min. The solution was kept at 40 °C throughout the experiment. 500 mM of iron (III) chloride ($FeCl_3.6H_2O$, Sigma Aldrich) solution was separately prepared and kept at 40 °C. The iron complex of Gel (Gel/Fe) or GelDA (GelDA/Fe) was simultaneously formed when the Gel or GelDA solution was mixed with iron chloride solution at a one-to-one volume ratio.

Polarization anisotropy measurement

Fluorescent agents were prepared by adding 10 μL of FITC-labeled dextran (10 mg/mL in 1XPBS) to 90 μL of $FeCl_3$ (500 mM in 1XPBS). This solution was then mixed with 100 μL of Gel or GelDA (10% (w/v) in 1XPBS). The fluorescence polarization was measured using a custom-built optical device.[29] We measured both the parallel (I_x) and perpendicular (I_y) components relative to the polarized excitation light and calculated the fluorescence anisotropy (r) from the ratiometry: $r = (I_x - I_y)\cdot(I_x + 2\cdot I_y)^{-1}$. Measurements were performed at room temperature.

Adhesion force measurement

Adhesion strength of Gel/Fe and GelDA/Fe was measured by lap shear test. The method was slightly modified from ASTM F2255-05.[18] 30 μL of Gel/Fe or GelDA/Fe complex was spread between two porcine skins (attached area: 1 cm × 1 cm) and kept for 10 min at room temperature. The force needed to detach the two skins at 1.3 mm/min of rate was continuously monitored by Instron (5848 Micro-tester) with a 10 N load cell.

Material characterization

The structure of Gel/Fe and GelDA/Fe were investigated by using HR-SEM (high-resolution scanning electron microscope, Zeiss Merlin). Lyophilized samples were coated with 20 nm of gold using a Denton Vacuum DV- 502A evaporator before imaging. For Fourier transform infrared spectroscopy (FT-IR) analysis, 7.5% (w/v) gelatin solution was measured using a Thermo Fisher Continuum FT-IR spectrometer before and after 1:1 (v/v) mixing with 250 mM $FeCl_3$.

In vivo degradation studies and histology

C57/BL6 (female, 4 months old) mice were used to perform degradation experiments. Gel/Fe and GelDA/Fe complex were prepared by mixing 50 μL of 15% (w/v) Gel or GelDA and 50 μL of 500 mM $FeCl_3$ in 1XPBS, respectively. The complexes were subcutaneously

implanted on the backs of mice. At 3 and 23 days post implantation, mice were euthanized. The implanted materials were harvested and weighed, and skin tissues surrounding the implants were collected for histology. The skin tissues were fixed with 10% formalin, paraffin embedded and sectioned (5 μm thickness). H&E staining was performed, and the slides were imaged by using Nanozoomer 2.0RS (Hamamatsu, Japan).

Cell viability

NIH 3T3 fibroblast cells were seeded in 96-well culture plates (~5×10^3 cells/well) and cultured for 24 hrs prior to use. The cell media was then replaced with media containing 10 mg/mL of GelDA and Gel. Cells were incubated for 1, 4 and 7 days, followed by analysis via the PrestoBlue® assay (Invitrogen), according to the manufacturer's instructions. Briefly, the PrestoBlue® reagent (20 μL) was added to each well after changing the media (200 μL) not containing any biopolymer. Fluorescence was measured at an excitation of 560 nm (10 nm bandwidth) and an emission at 590 nm (10 nm bandwidth) by using a Tecan Safire2 plate reader (Männedorf, Switzerland). Data were normalized by subtracting the baseline fluorescence of no-cell control wells.

Cell attachment test

NIH 3T3 cells (5×10^4 cells/scaffold) were seeded onto the GelDA/Fe fabricated on coverslips. Cells were stained with Acti-stain 488 phalloidin™ (Cytoskeleton, Inc) and DAPI (4′,6-diamidino-2-phenylindole, Sigma Aldrich) after 1, 4, or 7 days following the seeding. Before staining, cells were fixed in 4% (v/v) paraformaldehyde in PBS for 15 min, permeabilized in 0.1% (w/v) Triton X-100 (Sigma Aldrich) for 5 min, and then blocked in 1% (w/v) bovine serum albumin (BSA, Sigma Aldrich) for 30 min. Actin filaments were then stained in 200 nM Acti-stain™ in 0.1% BSA for 45 min, and nuclei were stained in 14.3 μM DAPI in PBS for 5 min. Stained cells were then imaged with a fluorescence microscope (Nikon Eclipse TE2000S).

Rapid dissolution of Gel/Fe and GelDA/Fe

Gel/Fe and GelDA/Fe complexes were prepared by mixing 50 μL of 15% (w/v) Gel or GelDA and 50 μL of 500 mM $FeCl_3$ in 1XPBS, respectively. After 5 minutes incubation at 37 °C, each complex was added to 3 mL of 1XPBS containing deferoxamine mesylate (Sigma Aldrich, 80 mg/mL), collagenase (from Clostridium histolyticum, Type XI, Sigma Aldrich, 1 mg/mL) or urokinase (from human urine, Alfa Aesar, 83,700 IU/mL) and kept at 37°C up to 1 hour.

Intestinal repair model

The murine small bowel was flushed with 1XPBS, and a small 3 mm incision was created with microscissors (n = 5). 15 μL of 15% (w/v) GelDA and 15 μL of 500 mM $FeCl_3$ in 1XPBS were applied and mixed at the injury site. After 5 minutes, the leak at the injury site was probed by injecting 200 μL of trypan blue dye as a bolus (<1 sec) through the intestinal loop with a diameter of ~2 mm. The flow rate was >12 mL/min, which is in the mid-range of physiological conditions between 2.5 mL/min in fasting subjects (i.e. those undergoing interventional procedures and being NPO) and 20 mL/min after meals.[30] Next, the glued

tissue was immersed in 3 mL of 80 mg/mL deferoxamine mesylate in 1XPBS and kept for 5 minutes at 37 °C. Leakage was re-assessed.

Uterine repair model

A surgical incision (2-4 mm) was made in one of the uterine horns, and 30 μL of 15% (w/v) GelDA and 30 μL of 500 mM $FeCl_3$ in 1XPBS were applied to repair the defect. Uterine potency was assessed by trypan blue injection. Mice (n = 5) were euthanized by compressed carbon dioxide using approved protocols. Animal experiments were performed in compliance with guidelines from the Institutional Subcommittee on Research Animal Care (Massachusetts General Hospital).

Supplementary Material

Refer to Web version on PubMed Central for supplementary material.

Acknowledgements

We are grateful to the following individuals: Yoshiko Iwamoto, for assistance in performing histology, Dr. Jun Seok Park for discussions on use of animal models and video editing and Dr. Jonathan Carlson for performing initial kinetic experiments. Part of this work was funded by R01EB010011 (RW). AK was supported by the Mac Erlaine Research Scholarship from the Academic Radiology Research Trust, St. Vincent's Radiology Group, Dublin, Ireland.

References

[1]. Shrikhande SV, DSouza MA. World J. Gastroenterol. 2008; 14:5789. [PubMed: 18855976]
[2]. Hii MW, Gyorki DE, Sakata K, Cade RJ, Banting SW. HPB (Oxford). 2011; 13:699. [PubMed: 21929670]
[3]. de Groof EJ, Cabral VN, Buskens CJ, Morton DG, Hahnloser D, Bemelman WA. Colorectal. Dis. 2016; 18:O119. [PubMed: 26847796]
[4]. Fuso L, Varone F, Nachira D, Leli I, Salimbene I, Congedo MT, Margaritora S, Granone P. Lung. 2016; 194:299. [PubMed: 26753560]
[5]. Eswara JR, Raup VT, Potretzke AM, Hunt SR, Brandes SB. Urology. 2015; 86:1228. [PubMed: 26368509]
[6]. Abel ME, Chiu YSY, Russell TR, Volpe PA. Dis. Colon Rectum. 1993; 36:447. [PubMed: 8482163]
[7]. Hjortrup A, Moesgaard F, Kjærgård J. Dis. Colon Rectum. 1991; 34:752. [PubMed: 1914738]
[8]. Suc B, Msika S, Fingerhut A, Fourtanier G, Hay J-M, Holmières F, Sastre B, Fagniez P-L. Ann. Surg. 2003; 237:57. [PubMed: 12496531]
[9]. D'Andrea AA, Costantino V, Sperti C, Pedrazzoli S. Ital. J. Gastroentrol. 1994; 26:283.
[10]. Koonce SL, Eck DL, Shaddix KK, Perdikis G. Ann. Plast. Surg. 2015; 74:107. [PubMed: 24905134]
[11]. Bornemann R, Koch EMW, Wollny M, Pflugmacher R. Eur. J .Orthop. Surg. Traumatol. 2014; 24:131.
[12]. Dimitrakakis G, von Oppell UO. Interact. Cardiovasc. Thorac. Surg. 2011; 13:118. [PubMed: 21775487]
[13]. Wood RE, Lacey SR, Azizkhan RG. J. Pediatr. Surg. 1992; 27:201. [PubMed: 1564619]
[14]. Wible BC, Gooden C, Saucier N, Borsa JJ, Cummings LS, Cho KH. J. Vasc. Interv. Radiol. 2014; 25:1821. [PubMed: 25442143]
[15]. Lee H, Scherer NF, Messersmith PB. Proc. Natl. Acad. Sci. 2006; 103:12999. [PubMed: 16920796]

[16]. Zaky M, El-Sayed1 MY, El-Megharbel SM, Taleb SA, Refat MS. J. Mex. Chem. Soc. 2014; 58:142.

[17]. D'Antonio MC, Wladimirsky A, Palacios D, Coggiola L, González-Baró AC, Baran EJ, Mercader RC. J. Braz. Chem. Soc. 2009; 20:445.

[18]. Lih E, Lee JS, Park KM, Park KD. Acta Biomater. 2012; 8:3261. [PubMed: 22617740]

[19]. Neilands JB. Annu. Rev. Biochem. 1981; 50:715. [PubMed: 6455965]

[20]. Tang S-H, Huang J-B. Acta Phys. Chim. Sin. 2001; 17:873.

[21]. Barrett DG, Fullenkamp DE, He L, Holten-Andersen N, Lee KYC, Messersmith PB. Adv. Funct. Mater. 2013; 23:1111. [PubMed: 23483665]

[22]. Meynard D, Babitt JL, Lin HY. Blood. 2014; 123:168. [PubMed: 24200681]

[23]. Annabi N, Nichol JW, Zhong X, Ji C, Koshy S, Khademhosseini A, Dehghani F. Tissue Eng. Part B Rev. 2010; 16:371. [PubMed: 20121414]

[24]. Koshy ST, Ferrante TC, Lewin SA, Mooney DJ. Biomaterials. 2014; 35:2477. [PubMed: 24345735]

[25]. Sun Z, Lv F, Cao L, Liu L, Zhang Y, Lu Z. Angew. Chem. Int. Ed. 2015; 54:7944.

[26]. Meddahi Pellé A, Legrand A, Marcellan A, Louedec L, Letourneur D, Leibler L. Angew. Chem. Int. Ed. 2014; 126:6487.

[27]. Rose S, Prevoteau A, Elzière P, Hourdet D, Marcellan A, Leibler L. Nature. 2014; 505:382. [PubMed: 24336207]

[28]. Grindy SC, Learsch R, Mozhdehi D, Cheng J, Barrett DG, Guan Z, Messersmith PB, Holten-Andersen N. Nat. Mater. 2015; 14:1210. [PubMed: 26322715]

[29]. Park KS, Huang C-H, Lee K, Yoo Y-E, Castro CM, Weissleder R, Lee H. Sci Adv. 2016; 2:e1600300.

[30]. Fine KD, Santa Ana CA, Porter JL, Fordtran JS. Gastroenterol. 1995; 108:983.

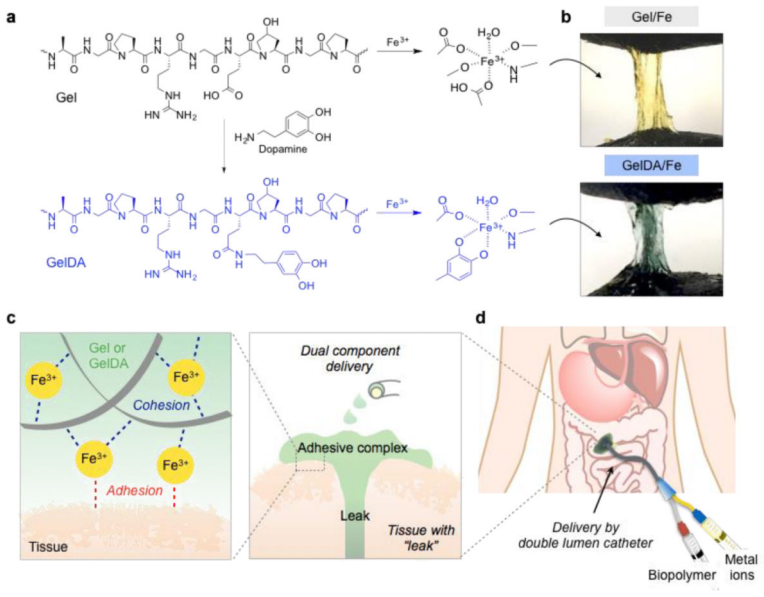

Fig. 1. Iron complexation of biopolymers yields metallo-bioadhesive

(a) Synthetic scheme starting with gelatin and/or dopamine modification. Note the Fe^{3+} complexation of either polymer with hexavalent coordination possibilities that extend beyond those shown. (b) Photographs of formed adhesive materials. (c) Fe^{3+} metal ions have a dual role in cohesion between strands of polymers and adhesion to tissue. (d) The two-component metallo-bioadhesive is delivered via dual lumen microcatheters where the components form the adhesive upon mixing at their delivery site.

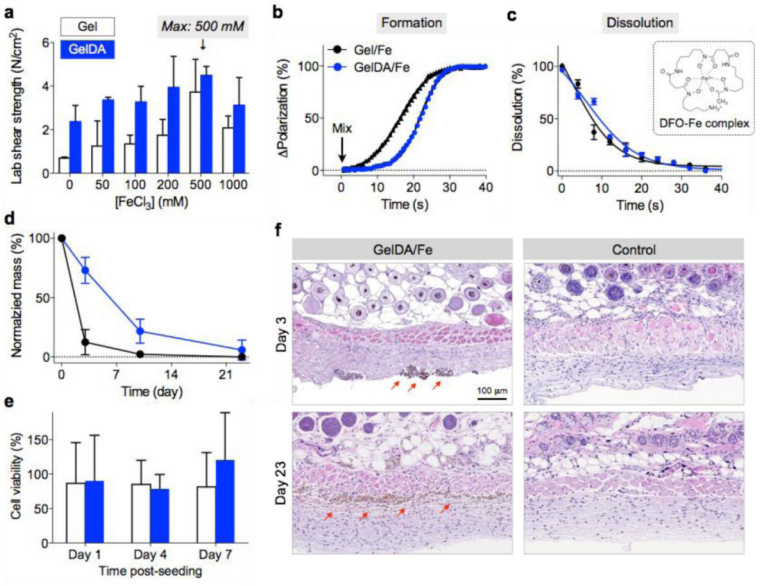

Fig. 2. Material characterization

(a) Lab shear strength of Gel/Fe and GelDA/Fe on porcine skin as a function of employed Fe concentration. Maximum strength is achieved at Fe concentrations around 500 mM (compare to Fig. S3). (b) Complexation time of Gel/Fe and GelDA/Fe as determined by fluorescence polarization change. Complexation and maximum adhesiveness are essentially complete within 30 seconds. (c) On demand dissolution of formed metallo-bioadhesives by incubaing them with the iron chelator deferoxamine (DFO). DFO efficiently complexes Fe from the formed metallo-adhesive and completely dissolves it within 30 seconds. (d) *In vivo* biodegradation of the formed metallo-bioadhesives after subcutaneous implantation. Both polymers are completely dissolved within 23 days though GelIDA has a slightly lower degradation rate compared to Gel. (e) Cell viability of NIH 3T3 fibroblast cells 1, 4, and 7 days after incubation with respective 10 mg/mL of biopolymers. There is no observed cytotoxicity. (f) H&E histology of tissue sections around the GelDA/Fe implantation site show no inflammation.

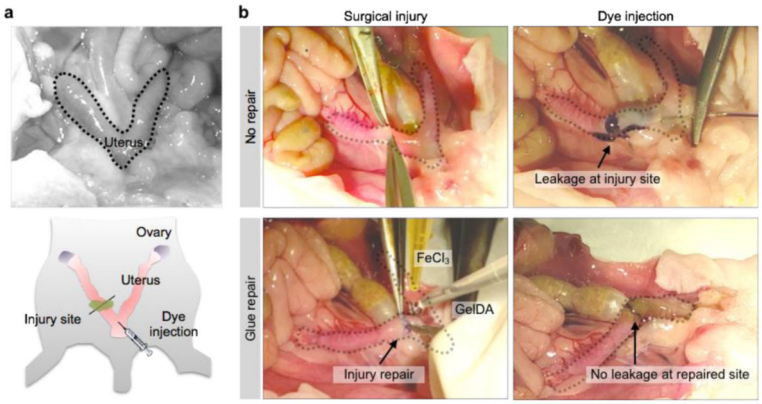

Fig. 3. In vivo repair of visceral injury

(a) Schematic illustration of the uterine injury model. (b) Top row shows the creation of uterine injury and testing by injection of trypan blue (note the extravasation). The bottom row shows the same experiment in a different animal but following glue application. The trypan blue does not leak. For additional models see Fig. S5.